

Correlations between Ca II H&K Emission and the Gaia M dwarf Gap

2 EMILY M. BOUDREAUX,<sup>1</sup> AYLIN GARCIA SOTO,<sup>1</sup> AND BRIAN C. CHABOYER<sup>1</sup>

3 <sup>1</sup>*Department of Physics and Astronomy, Dartmouth College, Hanover, NH 03755, USA*

4 (Received 02/07/2024; Revised 02/20/2024; Accepted 02/22/2024)

5 Submitted to ApJ

6 ABSTRACT

7 The Gaia M dwarf gap, also known as the Jao Gap, is a novel feature discovered in the Gaia DR2 G vs.  
8 BP-RP color magnitude diagram. This gap represents a 17 percent decrease in stellar density in a thin  
9 magnitude band around the convective transition mass ( $\sim 0.35M_{\odot}$ ) on the main sequence. Previous  
10 work has demonstrated a paucity of Hydrogen Alpha emission coincident with the G magnitude of  
11 the Jao Gap in the solar neighborhood. The exact mechanism which results in this paucity is as  
12 of yet unknown; however, the authors of the originating paper suggest that it may be the result of  
13 complex variations to a star's magnetic topology driven by the Jao Gap's characteristic formation and  
14 breakdown of stars' radiative transition zones. We present a follow up investigating another widely used  
15 magnetic activity metric, Calcium II H&K emission. Ca II H&K activity appears to share a similar  
16 anomalous behavior as H $\alpha$  does near the Jao Gap magnitude. We observe an increase in star-to-star  
17 variation of magnetic activity near the Jao Gap. We present a toy model of a stars magnetic field  
18 evolution which demonstrates that this increase may be due to stochastic disruptions to the magnetic  
19 field originating from the periodic mixing events characteristic of the convective kissing instabilities  
20 which drive the formation of the Jao Gap.

21 *Keywords:* Stellar Evolution (1599) — Stellar Evolutionary Models (2046)

22 1. INTRODUCTION

23 The initial mass requirements of molecular clouds col-  
24 lapsing to form stars results in a strong bias towards  
25 lower masses and later spectral classes during star for-  
26 mation. Partly as a result of this bias and partly as a  
27 result of their extremely long main-sequence lifetimes, M  
28 Dwarfs make up approximately 70 percent of all stars in  
29 the galaxy (Winters et al. 2019). Moreover, many planet  
30 search campaigns have focused on M Dwarfs due to the  
31 relative ease of detecting small planets in their habitable  
32 zones (e.g. Nutzman & Charbonneau 2008). M Dwarfs  
33 then represent both a key component of the galactic stel-  
34 lar population as well as the most numerous possible set  
35 of stars which may host habitable exoplanets. Given this  
36 key location M Dwarfs occupy in modern astronomy it

37 is important to have a thorough understanding of their  
38 structure and evolution.

39 Jao et al. (2018) discovered a novel feature in the Gaia  
40 Data Release 2 (DR2)  $G_{BP} - G_{RP}$  color-magnitude-  
41 diagram. Around  $M_G = 10$  there is an approximately  
42 17 percent decrease in stellar density of the sample of  
43 stars Jao et al. (2018) considered. Subsequently, this  
44 has become known as either the Jao Gap, or Gaia M  
45 Dwarf Gap. Following the initial detection of the Gap  
46 in DR2 the Gap has also potentially been observed in  
47 2MASS (Skrutskie et al. 2006; Jao et al. 2018); however,  
48 the significance of this detection is quite weak and it re-  
49 lies on the prior of the Gap's location from Gaia data.  
50 The Gap is also present in Gaia Early Data Release 3  
51 (EDR3) (Jao & Feiden 2021). These EDR3 and 2MASS  
52 data sets then indicate that this feature is not a bias  
53 inherent to DR2.

54 The Gap is generally attributed to convective instabil-  
55 ities in the cores of stars straddling the fully convective  
56 transition mass ( $0.3 - 0.35 M_{\odot}$ ) known as convective  
57 kissing instabilities (?Baraffe & Chabrier 2018). These

Corresponding author: Emily M. Boudreaux  
[emily.m.boudreaux.gr@dartmouth.edu](mailto:emily.m.boudreaux.gr@dartmouth.edu),  
[emily@boudreauxmail.com](mailto:emily@boudreauxmail.com)

instabilities interrupt the normal, slow, main sequence luminosity evolution of a star and result in luminosities lower than expected from the main sequence mass-luminosity relation (Jao & Feiden 2020).

The Jao Gap, inherently a feature of M Dwarf populations, provides an enticing and unique view into the interior physics of these stars (Feiden et al. 2021). This is especially important as, unlike more massive stars, M Dwarf seismology is infeasible due to the short periods and extremely small magnitudes which both radial and low-order low-degree non-radial seismic waves are predicted to have in such low mass stars (Rodríguez-López 2019). The Jao Gap therefore provides one of the only current methods to probe the interior physics of M Dwarfs.

The magnetic activity of M dwarfs is of particular interest due to the theorised links between habitability and the magnetic environment which a planet resides within (e.g. Lammer et al. 2012; Gallet et al. 2017; Kislyakova et al. 2017). M dwarfs are known to be more magnetically active than earlier type stars (Saar & Linsky 1985; Astudillo-Defru et al. 2017; Wright et al. 2018) while simultaneously this same high activity calls into question the canonical magnetic dynamo believed to drive the magnetic field of solar-like stars (the  $\alpha\Omega$  dynamo) (Shulyak et al. 2015). One primary challenge which M dwarfs pose is that stars less than approximately  $0.35 M_{\odot}$  are composed of a single convective region. This denies any dynamo model differential rotation between adjacent levels within the star. Alternative dynamo models have been proposed, such as the  $\alpha^2$  dynamo along with modifications to the  $\alpha\Omega$  dynamo which may be predictive of M dwarf magnetic fields (Chabrier & Küker 2006; Kochukhov 2021; Kleorin et al. 2023).

Despite this work, very few studies have dived specifically into the magnetic field of M dwarfs at or near the convective transition region. This is not surprising as that only spans approximately a 0.2 magnitude region in the Gaia BP-RP color magnitude diagram and is therefore populated by a relatively small sample of stars.

Jao et al. (2023) identify the Jao Gap as a strong discontinuity point for magnetic activity in M dwarfs. Two primary observations from their work are that the Gap serves as a boundary where very few active stars, in their sample of 640 M dwarfs, exist below the Gap and that the overall downward trend of activity moving to fainter magnitudes is anomalously high in within the 0.2 mag range of the Gap. Jao et al. Figures 3 and 13 make this paucity in H $\alpha$  emission particularly clear. Based on previous work from Spada & Lanzafame (2020); Curtis et al. (2020); Dungee et al. (2022) the authors propose that the mechanism resulting in the reduced fraction of

active stars within the Gap is that as the radiative zone dissipates due to core expansion, angular momentum from the outer convective zone is dumped into the core resulting in a faster spin down than would otherwise be possible. Effectively the core of the star acts as a sink, reducing the amount of angular momentum which needs to be lost by magnetic braking for the outer convective region to reach the same angular velocity. Given that H $\alpha$  emission is strongly coupled magnetic activity in the upper chromosphere (Newton et al. 2016; Kumar et al. 2023) and that a star’s angular velocity is a primary factor in its magnetic activity, a faster spin down will serve to more quickly dampen H $\alpha$  activity.

In addition to H $\alpha$  the Calcium Fraunhofer lines may be used to trace the magnetic activity of a star. These lines originate from magnetic heating of the lower chromosphere driven by magnetic shear stresses within the star. Both Perdelwitz et al. (2021) and Boudreaux et al. (2022) present calcium emission measurements for stars spanning the Jao Gap. In this paper we search for similar trends in the Ca II H& K emission as Jao et al. see in the H $\alpha$  emission. In Section 2 we investigate the empirical star-to-star variability in emission and quantify if this could be due to noise or sample bias; in Section 3 we present a simplified toy model which shows that the mixing events characteristic of convective kissing instabilities could lead to increased star-to-star variability in activity as is seen empirically.

## 2. CORRELATION

Using Ca II H&K emission data from Perdelwitz et al. (2021) and Boudreaux et al. (2022) (quantified using the  $R'_{HK}$  metric Middelkoop 1982; Rutten 1984) we investigate the correlation between the Jao Gap magnitude and stellar magnetic activity. We are more statistically limited here than past authors have been due to the requirement for high resolution spectroscopic data when measuring Calcium emission.

The merged dataset is presented in Figure 1. The sample overlap between Perdelwitz et al. (2021) and Boudreaux et al. (2022) is small (only consisting of five targets). For those five targets there is an approximately 1.5 percent average difference between measured  $\log(R'_{HK})$  values, with measurements from Boudreaux et al. biased to be slightly more negative than those from Perdelwitz et al.

There is a visual discontinuity in the spread of stellar activity below the Jao Gap magnitude. Further discussion of why there may be disagreement between the observed magnitude of the gap and the discontinuity which we identify may be found in Section 2.1. In order to quantify the significance of this discontinuity we mea-

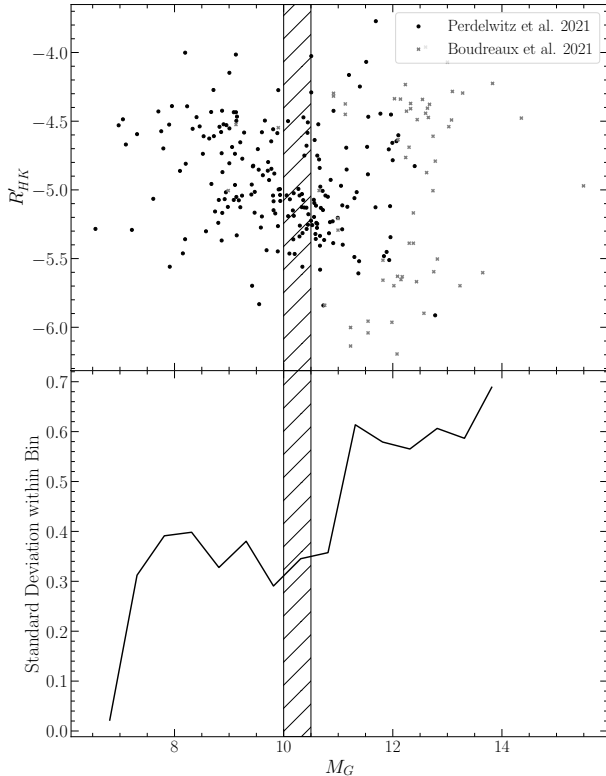


**Figure 1.** Merged Dataset from [Perdelwitz et al. \(2021\)](#); [Boudreaux et al. \(2022\)](#). Note the increase in the spread of  $R'_{HK}$  around the Jao Gap Magnitude (top). Standard deviation of Calcium emission data within each bin. Note the discontinuity near the Jao Gap Magnitude (bottom). The location of the Gap as identified in literature is shown by the hatched region ( $\sim 10$ - $10.5 M_G$ ). Potential explanations for the disagreement in magnitude are discussed in detail in Section 2.1.

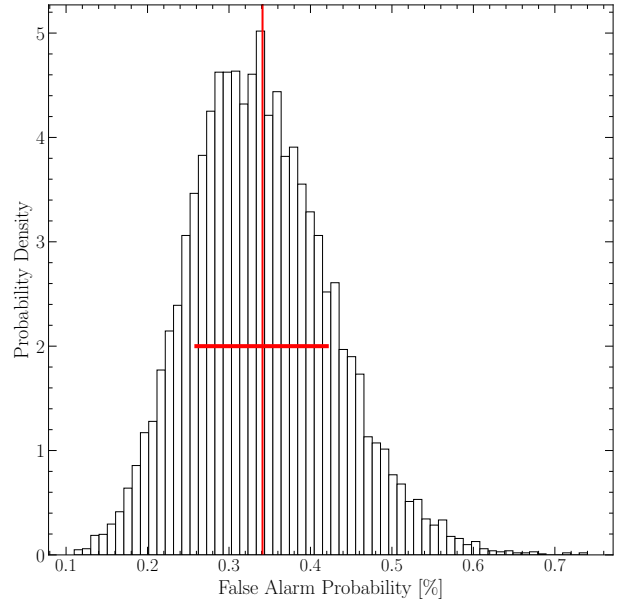


**Figure 2.** Probability distribution of the false alarm probability for the discontinuity seen in Figure 1. The mean of this distribution is  $0.341\% \pm 0.08$ .

161 sure the false alarm probability of the change in standard  
 162 deviation.

163 First we split the merged dataset into bins with a  
 164 width of 0.5 mag. In each bin we measure the stan-  
 165 dard deviation about the mean of the data. The results  
 166 of this are shown in Figure 1 (bottom). In order to mea-  
 167 sure the false alarm probability of this discontinuity we  
 168 first resample the merged calcium emission data based  
 169 on the associated uncertainties for each datum as pre-  
 170 sented in their respective publications. Then, for each  
 171 of these “resample trials” we measure the probability  
 172 that a change in the standard deviation of the size seen  
 173 would happen purely due to noise. Results of this test  
 174 are show in in Figure 2.

175 This rapid increase star-to-star variability would only  
 176 arise due purely to noise  $0.3 \pm 0.08$  percent of the time  
 177 and is therefore likely either a true effect or an alias of  
 178 some sample bias.

179 If the observed increase in variability is not due to a  
 180 sample bias and rather is a physically driven effect then  
 181 there is an obvious similarity between these findings and  
 182 those of [Jao et al. \(2023\)](#). Specifically we find a increase  
 183 in variability below the magnitude of the Gap. More-  
 184 over, this variability increase is primarily driven by an  
 185 increase in the number of low activity stars (as opposed  
 186 to an increase in the number of high activity stars). We  
 187 can further investigate the observed change in variability  
 188 for only low activity stars by filtering out those stars at  
 189 or above the saturated threshold for magnetic activity.  
 190 [Boudreaux et al. \(2022\)](#) identify  $\log(R'_{HK}) = -4.436$   
 191 as the saturation threshold. We adopt this value and  
 192 filter out all stars where  $\log(R'_{HK}) \geq -4.436$ . Apply-  
 193 ing the same analysis to this reduced dataset as was  
 194 done to the full dataset we still find a discontinuity at  
 195 the same location (Figure 3). This discontinuity is of a  
 196 smaller magnitude and consequently is more likely to be  
 197 due purely to noise, with a  $7 \pm 0.2$  percent false alarm  
 198 probability. This false alarm probability is however only  
 199 concerned with the first point after the jump in vari-  
 200 ability. If we consider the false alarm probability of the  
 201 entire high variability region then the probability that  
 202 the high variability region is due purely to noise drops  
 203 to  $1.4 \pm 0.04$  percent.

204 Further, various authors have shown that the strength  
 205 of Calcium II H&K emission may evolve over month to  
 206 year timescales (e.g. [Rauscher & Marcy 2006](#); [Perdel-  
 207 witz et al. 2021](#); [Cretignier et al. 2024](#)). Targets from  
 208 [Boudreaux et al. \(2022\)](#) were observed an average of

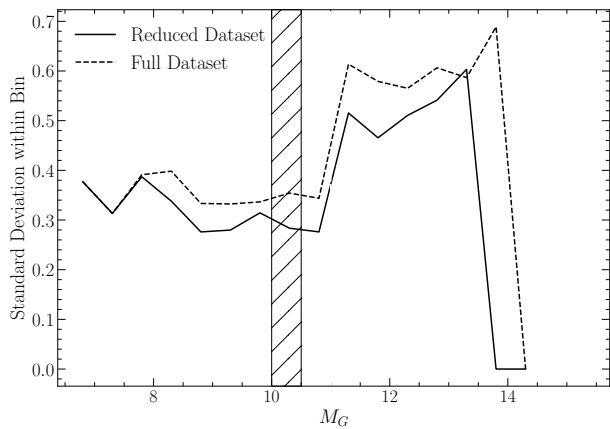


**Figure 3.** Spread in the magnetic activity metric for the merged sample with any stars  $\log(R'_{HK}) > -4.436$  filtered out. The location of the Gap as identified in literature is shown by the hatched region ( $\sim 10$ - $10.5 M_G$ ).

only four times and over year long timescales. Therefore, the nominal  $\log(R'_{HK})$  values derived in that work may be biased by stellar variability. However, the scale of observed variability in the activity metric is significantly smaller than the star-to-star activity variability addressed here and therefore activity cycles are not expected to be of particular relevance. Specifically, the amplitude of variability is generally  $\Delta \log(R'_{HK}) \lesssim 0.2$  whereas in this work we address variability on the order of  $\Delta \log(R'_{HK}) \lesssim 2$ .

We observe a strong, likely statistically significant, discontinuity in the star-to-star variability of Ca II H&K emission below the magnitude of the Jao Gap. However, modeling is required to determine if this discontinuity may be due to the same underlying physics.

### 2.1. Coincidence with the Jao Gap Magnitude

While the observed increase in variability seen here does not seem to be coincident with the Jao Gap — instead appearing to be approximately 0.5 mag fainter, in agreement with what is observed in Jao et al. (2023) — a number of complicating factors prevent us from falsifying that these two features are not coincident. Jao et al. find, similar to the results presented here, that the paucity of  $H\alpha$  emission originates below the Gap. Moreover, we use a 0.5 magnitude bin size when measuring the star-to-star variability which injects error into the positioning of any feature in magnitude space. We can quantify the degree of uncertainty the magnitude bin choice injects by conducting Monte Carlo trials where bins are randomly shifted redder or bluer. We conduct 10,000 trials where each trial involves sampling a random shift to the bin start location from a normal distribution with a standard deviation of 1 magnitude.

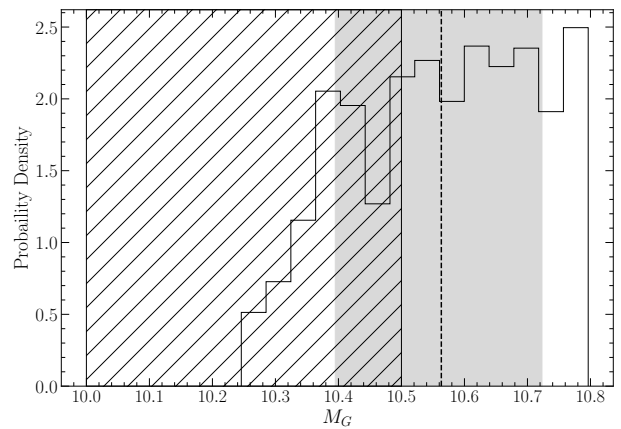


**Figure 4.** Probability density distribution of discontinuity location as identified in the merged dataset. The dashed line represents the mean of the distribution while the shaded region runs from the 16th percentile to the 84th percentile of the distribution. This distribution was built from 10,000 independent samples where the discontinuity was identified as the highest value in the gradient of the standard deviation. The location of the Gap as identified in literature is shown by the hatched region ( $\sim 10$ - $10.5 M_G$ ).

For each trial we identify the discontinuity location as the maximum value of the gradient of the standard deviation (this is the derivative of the data in Figures ?? & 3). Some trials result in the maximal value lying at the 0th index of the magnitude array due to edge effects, these trials are rejected (and account for 11% of the trials). The uncertainty in the identified magnitude of the discontinuity due to the selected start point of the magnitude bins reveals a  $1\sigma = \pm 0.32$  magnitude uncertainty in the location of the discontinuity (Figure 4). Finally, all previous studies of the M dwarf Gap (Jao et al. 2018; Jao & Feiden 2021; Mansfield & Kroupa 2021; Boudreaux et al. 2022; Jao et al. 2023) demonstrate that the Gap has a color dependency, shifting to fainter magnitudes as the population reddens and consequently an exact magnitude range is ill-defined. Therefore we cannot falsify the model that the discontinuity in star-to-star activity variability is coincident with the Jao Gap magnitude.

### 2.2. Rotation

It is well known that star's magnetic activity tend to be correlated with their rotational velocity (Vaughan et al. 1981; Newton et al. 2016; Astudillo-Defru et al. 2017; Houdebine et al. 2017; Boudreaux et al. 2022); therefore, we investigate whether there is a similar correlation between Gap location and rotational period in our dataset. All targets from Boudreaux et al. (2022) already have published rotational periods; however, targets from Perdelwitz et al. (2021) do not necessarily have

published periods. Therefore, we derive photometric rotational periods for these targets here. Given the inherent heterogeneity of M Dwarf stellar surfaces (Boisse et al. 2011; Robertson et al. 2020) we are able to determine the rotational period of a star through the analysis of active regions. Various methodologies can be employed for this purpose, including the examination of photometry and light curves (e.g., Newton et al. 2016), and the observation of temporal changes in the strength of chromospheric emission lines such as Ca II H & K or H $\alpha$  (e.g., Fuhrmeister et al. 2019; Kumar & Fares 2023). In this work, new rotational periods are derived from TESS 2-minute cadence data<sup>1</sup>.

Due to both the large frequency and amplitudes of M dwarf flaring rates the photometric period can prove difficult to measure — as frequency directly correlates with periodicity. Thus, following the process described in García Soto et al. (2023), we utilize two methods in this paper to reduce the effect of flares. One method uses *stella* a python package which implements a series of pre-trained convolutional neural networks (CNNs) to remove flare-shaped features in a light curve (Feinstein et al. 2020a). The second method separates a star’s photometry into 10 minute bins to account for misshapen flares which *stella* is known to be biased against detecting.

*stella* employs a diverse library of models trained with varying initial seeds (Feinstein et al. 2020b,a). The Convolutional Neural Networks in *stella* are trained on labeled TESS 2-min for both flares and non-flares. For the purposes of this paper, we use an ensemble of 100 models in *stella*’s library to optimize model performance (Feinstein et al. 2020b, for further detail). *stella* scores flairs with a probability of between 0 to 1 — where higher values indicate a higher confidence that a feature is a flare. Here we adopt a score of 0.5 as the cutoff threshold, all features with a score of 0.5 or greater are classed as flares and removed (e.g. Feinstein et al. 2020b).

Furthermore, we also bin the data from a 2-min to 10-min cadence using the python package *lightkurve*’s binning function (Lightkurve Collaboration et al. 2018; Barentsen et al. 2020). This further reduces any flaring-contribution that might have been missed by *stella*<sup>2</sup>. Subsequently, we filter photometry, only retaining data whos residuals are less than 4 times the root-mean-square deviation.

<sup>1</sup> Some M Dwarfs lacking a documented rotational period did not have sufficient TESS data to yield fiducial rotational periods

<sup>2</sup> This is relevant for flares that are misshapen at the start or break in the dataset due to missing either the ingress or egress.

Gaussian processes for modeling the periods are based on Angus et al. (2018) for the subset of M Dwarfs with no fiducial periods. The *starspot* package is adapted for light curve analysis (Angus 2021; Angus & Garcia Soto 2023). Our Gaussian process kernel function incorporates two stochastically-driven simple harmonic oscillators, representing primary ( $P_{rot}$ ) and secondary ( $P_{rot}/2$ ) rotation modes. First, we implement the Lomb-Scargle periodogram within *starspot* to initially estimate the period. After which, we create a maximum a posteriori (MAP) fit using *starspot* to generate a model for stellar rotation. To obtain the posterior of the stellar rotation model, we use Markov Chain Monte Carlo (MCMC) sampling using the *pymc3* package (Salvatier et al. 2016) within our adapted *starspot* version. All rotational periods are presented in Table 1. Our final sample contains 187 stars with measured rotational periods. We derive new rotational periods for 7 of these.

One might expect a decrease in mean rotational period around the magnitude of the Gap, due to the slight decrease in magnetic activity. However, there is no statistically significant correlation between rotational period and G magnitude which we can detect given our sample size (Figure 5). Rotational period is however, not the ideal parametrization to use, as magnetic activity is more directly related to the Rossby number ( $Ro$ ). Using the empirical calibration presented in Wright et al. (2018) (Equation 1) we find the mixing timescale for each star such that the Rossby Number is defined as  $Ro = P_{rot}/\tau_c$ .

$$\tau_c = 0.64 + 0.25 * (V - K) \quad (1)$$

When we compare Rossby number to G magnitude (Figure 6) we find that there may be a slight paucity of rotation coincident with the decrease in spread of the activity metric. We quantify the statistical significance of this drop by building a Gaussian kernel density estimator (kde) based on the data outside of this range, and then resampling that kde 10000 times for each data point in the theorized paucity range. The false alarm probability that that drop is due to noise is then the product of the fraction of samples which are less than or equal to the value of each data point. We find that there is a 0.022 percent probability that this dip is due purely to noise.

### 2.3. Limitations

There are two primary limitation of our dataset. First, we only have 264 star in our dataset (with measured  $R'_{HK}$ , 187 with rotational periods) limiting the statistical power of our analysis. This is primarily due to the relative difficulty of obtaining Ca II H&K measure-

ID	G Mag	V Mag	K Mag	$\log(R'_{HK})$	$e\_Log(R'_{HK})$	Ro	prot	r_prot
	mag	mag	mag				d	
2MASS J00094508-4201396	12.14	13.659	8.223	-4.339	0.001	0.009	0.859	Bou22
2MASS J00310412-7201061	12.301	13.648	8.445	-5.388	0.003	0.928	80.969	Bou22
2MASS J01040695-6522272	12.447	13.95	8.532	-4.489	0.001	0.006	0.624	Bou22
2MASS J02004725-1021209	12.778	14.113	9.092	-4.791	0.001	0.188	14.793	Bou22
2MASS J02014384-1017295	13.026	14.477	9.189	-4.54	0.001	0.034	3.152	Bou22
2MASS J02125458+0000167	12.096	13.58	8.168	-4.635	0.001	0.048	4.732	Bou22
2MASS J02411510-0432177	12.251	13.79	8.246	-4.427	0.001	0.004	0.4	Bou22
2MASS J03100305-2341308	12.23	13.5	8.567	-4.234	0.001	0.028	2.083	Bou22
2MASS J03205178-6351524	12.087	13.433	8.195	-5.629	0.004	1.029	91.622	Bou22
2MASS J05015746-0656459	10.649	12.196	6.736	-5.005	0.002	0.875	88.5	Bou22

**Table 1.** First 10 rows of the dataset used in this work. This data is available as a machine readable supliment to this article.

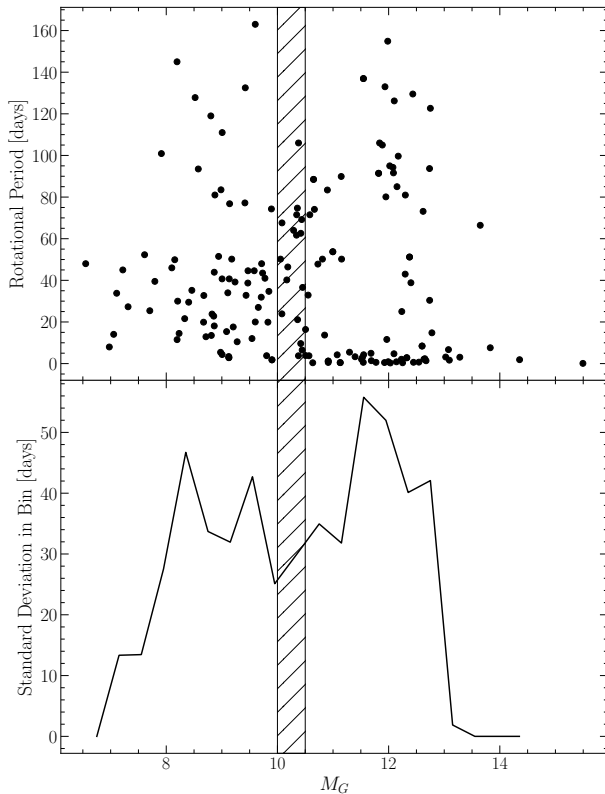


**Figure 5.** Rotational Periods against G magnitude for all stars with rotational periods (top). Standard deviation of rotational period within magnitude bin (bottom). The location of the Gap as identified in literature is shown by the hatched region ( $\sim 10-10.5 M_G$ ).

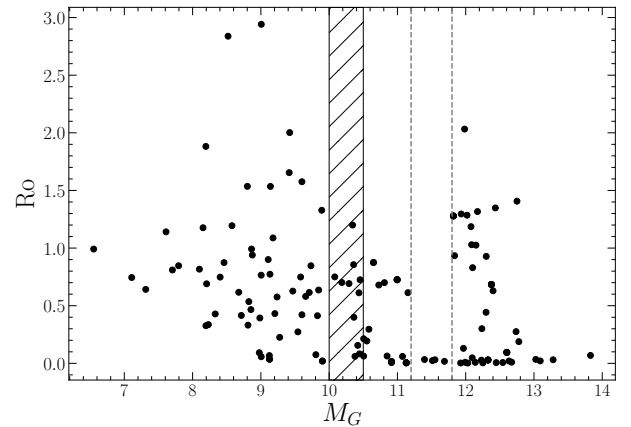


**Figure 6.** Rossby number vs. G magnitude for all stars with rotational periods and V-K colors on Simbad. Dashed lines represent the hypothesized region of decreased rotation. The location of the Gap as identified in literature is shown by the hatched region ( $\sim 10-10.5 M_G$ ).

367 ments compared to obtaining  $H\alpha$  measurements. Re-

368 liable measurements require both high spectral resolu-

369 tions ( $R \sim 16000$ ) and a comparatively blue wavelength  
370 range<sup>3</sup>.

371 Additionally, the sample we do have does not extend  
372 to as low mass as would be ideal. This presents a degeneracy  
373 between two potential causes for the observed in-  
374 creased star-to-star variability. One option, as presented

<sup>3</sup> wrt. to what many spectrographs cover. There is no unified resource listing currently commissioned spectrographs; however, it is somewhat hard to source glass which transmits well at H&K wavelengths limiting the lower wavelength of most spectrographs.

above and elaborated on in the following section, is that this is due to kissing instabilities. However, another possibility is that this increased variability is intrinsic to the magnetic fields of fully convective stars. This alternate option may be further supported by the shape of the magnetic activity spread vs. G magnitude relation. Convective kissing instabilities are not expected to continue to much lower masses than the fully convective transition mass. The fact that the increase in variance which we observe continues to much fainter magnitudes would therefore be somewhat surprising in a purely convective kissing instability driven framework (though the degeneracy between potentially physically driven increase in variance and increase in variance due to the noise-magnitude relation complicates attempts to constrain this.) There is limited discussion in the literature of overall magnetic field strength spanning the fully convective transition mass; however, Shulyak et al. (2019) present estimated magnetic field strengths for 47 M dwarfs, spanning a larger area around the convective transition region and their dataset does not indicate a inherently increased variability for fully convective stars.

### 3. MODELING

One of the most pressing questions related to this work is whether or not the increased star-to-star variability in the activity metric and the Jao Gap, which are coincident in magnitude, are driven by the same underlying mechanism. The challenge when addressing this question arises from current computational limitations. Specifically, the kinds of three dimensional magneto-hydrodynamical simulations — which would be needed to derive the effects of convective kissing instabilities on the magnetic field of the star — are infeasible to run over gigayear timescales while maintaining thermal timescale resolutions needed to resolve periodic mixing events.

In order to address this and answer the specific question of *could kissing instabilities result in increased star-to-star variability of the magnetic field*, we adopt a very simple toy model. Kissing instabilities result in a transient radiative zone separating the core of a star (convective) from its envelope (convective). When this radiative zone breaks down two important things happen: one, the entire star becomes mechanically coupled, and two, convective currents can now move over the entire radius of the star. Jao et al. (2023) propose that this mechanical coupling may allow the star’s core to act as an angular momentum sink thus accelerating a stars spin down and resulting in anomalously low H $\alpha$  emission.

Regardless of the exact mechanism by which the magnetic field may be affected, it is reasonable to expect that both the mechanical coupling and the change to

the scale of convective currents will have some effect on the star’s magnetic field. On a microscopic scale both of these will change how packets of charge within a star move and may serve to disrupt a stable dynamo. Therefore, in the model we present here we make only one primary assumption: *every mixing event may modify the star’s magnetic field by some amount*. Within our model this assumption manifests as a random linear perturbation applied to some base magnetic field at every mixing event. The strength of this perturbation is sampled from a normal distribution with some standard deviation,  $\sigma_B$ .

Synthetic stars are sampled from a grid of stellar models evolved using the Dartmouth Stellar Evolution Program (DSEP) with similar parameters to those used in Boudreaux & Chaboyer (2023). Each stellar model was evolved using a high temporal resolution (timesteps no larger than 10,000 years) and typical numerical tolerances of one part in  $10^5$ . Each model was based on a GS98 (Grevesse & Sauval 1998) solar composition with a mass range from  $0.3 M_{\odot}$  to  $0.4 M_{\odot}$ . Finally, models adopt OPLIB high temperature radiative opacities, Ferguson 2004 low temperature radiative opacities, and include both atomic diffusion and gravitational settling. A Kippenhan-Iben diagram showing the structural evolution of a model within the Gap is shown in Figure 7.

Each synthetic star is assigned some base magnetic activity ( $B_0 \sim \mathcal{N}(1, \sigma_B)$ ) and then the number of mixing events before some age  $t$  are counted based on local maxima in the core temperature. The toy magnetic activity at age  $t$  for the model is given in Equation 2. An example of the magnetic evolution resulting from this model is given in Figure 8. Fundamentally, this model presents magnetic activity variation due to mixing events as a random walk and therefore results will increasing divergence over time.

$$B(t) = B_0 + \sum_i B_i \sim \mathcal{N}(1, \sigma_B) \quad (2)$$

Applying the same analysis to these models as was done to the observations as described in Section 2 we find that this simple model results in a qualitatively similar trend in the standard deviation vs. Magnitude graph (Figure 9). In order to reproduce the approximately 50 percent change to the spread of the activity metric observed in the combined dataset in section 2 a distribution with a standard deviation of 0.1 is required when sampling the change in the magnetic activity metric at each mixing event. This corresponds to 68 percent of mixing events modifying the activity strength by 10 percent or less. The interpretation here is important: what

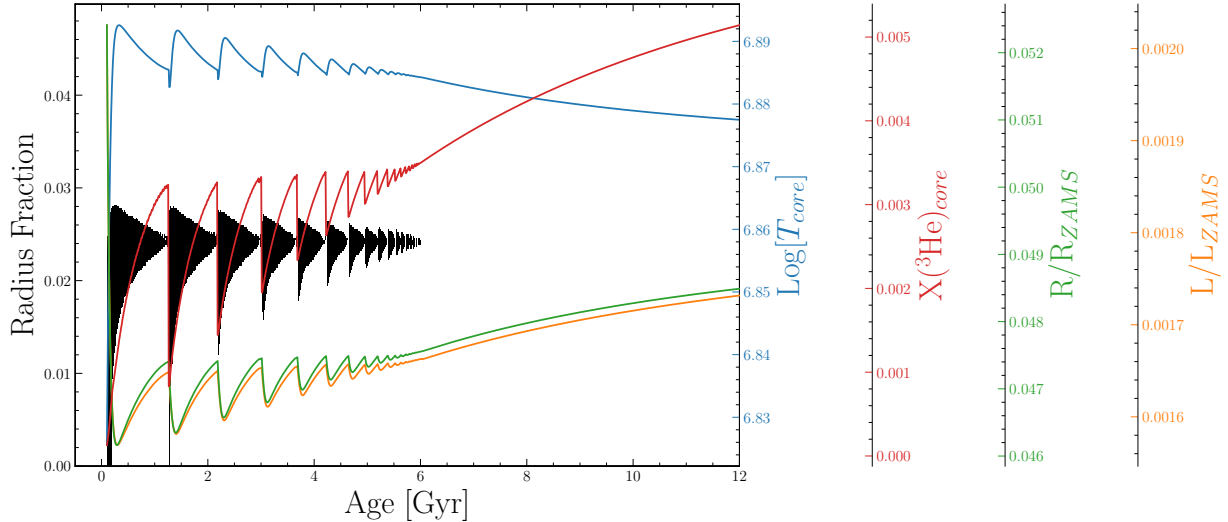


**Figure 7.** Kippenhan-Iben diagram for a 0.345 solar mass star. Note the periodic mixing events (where the plotted curves peak).

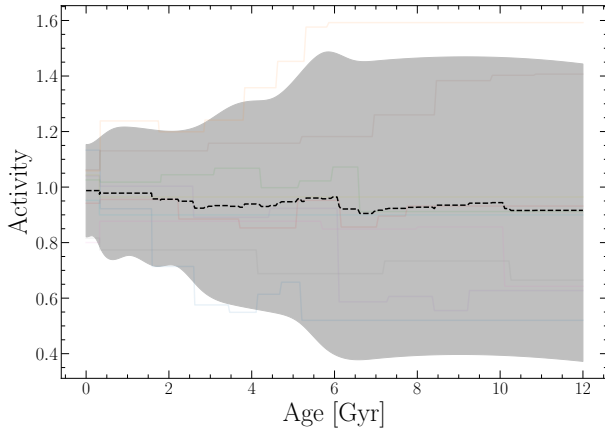


**Figure 8.** Example of the toy model presented here resulting in increased divergence between stars magnetic fields. The shaded region represents the maximum spread in the two point correlation function at each age.

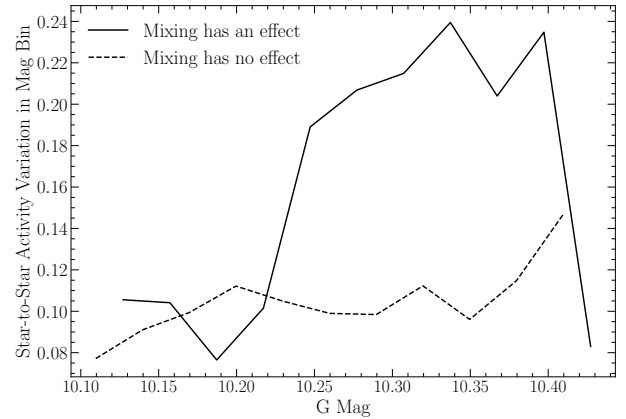


**Figure 9.** Toy model results showing a qualitatively similar discontinuity in the star-to-star magnetic activity variability.

475 this qualitative similarity demonstrates is that it may be  
 476 reasonable to expect kissing instabilities to result in the  
 477 observed increased star-to-star variation. Importantly,  
 478 we are not able to claim that kissing instabilities *do* lead  
 479 to these increased variations, only that they reasonably  
 480 could. Further modeling, observational, and theoretical  
 481 efforts will be needed to more definitively answer this  
 482 question.

### 483 3.1. Limitations

484 The model presented in this paper is very limited and  
 485 it is important to keep these limitations in mind when in-  
 486 terpreting the results presented here. Some of the main  
 487 challenges which should be leveled at this model are the  
 488 assumption that the magnetic field will be altered by

489 some small random perturbation at every mixing event.  
 490 This assumption was informed by the large number of  
 491 free parameters available to a physical star during the  
 492 establishment of a large scale magnetic field and the as-  
 493 sociated likely stochastic nature of that process. How-  
 494 ever, it is similarly believable that the magnetic field  
 495 will tend to alter in a uniform manner at each mixing  
 496 event. For example, since differential rotation is gener-  
 497 ally proportional to the temperature gradient within a  
 498 star and activity is strongly coupled to differential rota-  
 499 tion then it may be that as the radiative zone reforms  
 500 over thermal timescales the homogenization of angular  
 501 momentum throughout the star results in overall lower  
 502 amounts of differential rotation each after mixing event  
 503 than would otherwise be present.

504 Moreover, this model does not consider how other de-  
 505 generate sources of magnetic evolution such as stellar



506 spin down, relaxation, or coronal heating may effect  
 507 star-to-star variability. These could conceivably lead to  
 508 a similar increase in star-to-star variability which is co-  
 509 incident with the Jao Gap magnitude as the switch from  
 510 fully to partially convective may effect efficiency of these  
 511 process.

512 Additionally, there are challenges with this toy model  
 513 that originate from the stellar evolutionary model. Ob-  
 514 servations of the Jao Gap show that the feature is not  
 515 perpendicular to the magnitude axis; rather, it is in-  
 516 versely proportional to the color. No models of the Jao  
 517 Gap published at the time of writing capture this color  
 518 dependency and *what causes this color dependency* re-  
 519 mains one of the most pressing questions relating to the  
 520 underlying physics. This non captured physics is one  
 521 potential explanation for why the magnitude where our  
 522 model predicts the increase in variability is not in agree-  
 523 ment with where the variability jump exists in the data.

524 Finally, we have not considered detailed descriptions  
 525 of the dynamos of stars. The magnetohydrodynamical  
 526 modeling which would be required to model the evolu-  
 527 tion of the magnetic field of these stars at thermal  
 528 timescale resolutions over gigayears is currently beyond  
 529 the ability of practical computing. Therefore future  
 530 work should focus on limited modeling which may in-  
 531 form the evolution of the magnetic field directly around  
 532 the time of a mixing event.

533 4. CONCLUSION

534 It is, at this point, well established that the Jao Gap  
 535 may provide a unique view of the interiors of stars for  
 536 which other probes, such as seismology, fail. However, it  
 537 has only recently become clear that the Gap may lend  
 538 insight into not just structural changes within a star  
 539 but also into the magnetic environment of the star. *Jao*  
 540 *et al. (2023)* presented evidence that the physics driv-  
 541 ing the Gap might additionally result in a paucity of  
 542 H $\alpha$  emission. These authors propose potential physical

543 mechanisms which could explain this paucity, including  
 544 the core of the star acting as an angular momentum sink  
 545 during mixing events.

546 Here we have expanded upon this work by probing  
 547 the degree and variability of Calcium II H&K emission  
 548 around the Jao Gap. We lack the same statistical power  
 549 of *Jao et al.*'s sample; however, by focusing on the star-  
 550 to-star variability within magnitude bins we are able  
 551 to retain statistical power. We find that there is an  
 552 anomalous increase in variability at a G magnitude of  
 553  $\sim 11$ . This is only slightly below the observed mean gap  
 554 magnitude.

555 Additionally, we propose a simple model to explain  
 556 this variability. Making the assumption that the peri-  
 557 odic convective mixing events will have some small but  
 558 random effect on the overall magnetic field strength we  
 559 are able to qualitatively reproduce the increase activity  
 560 spread in a synthetic population of stars.

561 This work has made use of the NASA astrophysical  
 562 data system (ADS). We would like to thank Elisabeth  
 563 Newton, Aaron Dotter, and Gregory Feiden for their  
 564 support and for useful discussion related to the topic of  
 565 this paper. Additionally, we would like to thank Keigh-  
 566 ley Rockcliffe, Kara Fagerstrom, and Isabel Halstead for  
 567 their useful discussion related to this work. Finally, we  
 568 would like to thank the referee for their careful reading  
 569 and critique of this article. We acknowledge the support  
 570 of a NASA grant (No. 80NSSC18K0634).

571 *Software:* The Dartmouth Stellar Evolution Program  
 572 (DSEP) (*Dotter et al. 2008*), *BeautifulSoup* (*Richardson*  
 573 *2007*), *mechanize* (*Chandra&Varanasi2015*), *FreeEOS* (*Ir-*  
 574 *win 2012*), *pyTOPSScrape* (*Boudreaux 2022*), *lightkurve*  
 575 (*Lightkurve Collaboration et al. 2018*), *stella* (*Feinstein*  
 576 *et al. 2020a*), *starspot* (*Angus 2021; Angus & Garcia Soto*  
 577 *2023*)

REFERENCES

578 Angus, R. 2021, Zenodo, doi: [10.5281/zenodo.4613887](https://doi.org/10.5281/zenodo.4613887)  
 579 Angus, R., & Garcia Soto, A. 2023,  
 580 *agarciasoto18/starrotate: Alternate Starrotate for Paper,*  
 581 *v1.1.1*, Zenodo, doi: [10.5281/zenodo.7697238](https://doi.org/10.5281/zenodo.7697238)  
 582 Angus, R., Morton, T., Aigrain, S., Foreman-Mackey, D., &  
 583 Rajpaul, V. 2018, *Monthly Notices of the Royal*  
 584 *Astronomical Society*, 474, 2094,  
 585 doi: [10.1093/mnras/stx2109](https://doi.org/10.1093/mnras/stx2109)  
 586 Astudillo-Defru, N., Delfosse, X., Bonfils, X., et al. 2017,  
 587 *A&A*, 600, A13, doi: [10.1051/0004-6361/201527078](https://doi.org/10.1051/0004-6361/201527078)  
 588 Baraffe, I., & Chabrier, G. 2018, *A&A*, 619, A177,  
 589 doi: [10.1051/0004-6361/201834062](https://doi.org/10.1051/0004-6361/201834062)  
 590 Barentsen, G., Hedges, C., Vinícius, Z., et al. 2020,  
 591 *KeplerGO/Lightkurve: Lightkurve v1.11.0*, Zenodo,  
 592 doi: [10.5281/zenodo.3836658](https://doi.org/10.5281/zenodo.3836658)  
 593 Boisse, I., Bouchy, F., Hébrard, G., et al. 2011, *A&A*, 528,  
 594 A4, doi: [10.1051/0004-6361/201014354](https://doi.org/10.1051/0004-6361/201014354)  
 595 Boudreaux, E. M., & Chaboyer, B. C. 2023, *ApJ*, 944, 129,  
 596 doi: [10.3847/1538-4357/acb685](https://doi.org/10.3847/1538-4357/acb685)

- 597 Boudreaux, E. M., Newton, E. R., Mondrik, N.,  
 598 Charbonneau, D., & Irwin, J. 2022, *ApJ*, 929, 80,  
 599 doi: [10.3847/1538-4357/ac5cbf](https://doi.org/10.3847/1538-4357/ac5cbf)
- 600 Boudreaux, T. 2022, *tboudreaux/pytopsscrape*:  
 601 *pyTOPSScrape v1.0*, v1.0, Zenodo,  
 602 doi: [10.5281/zenodo.7094198](https://doi.org/10.5281/zenodo.7094198)
- 603 Chabrier, G., & Küker, M. 2006, *A&A*, 446, 1027,  
 604 doi: [10.1051/0004-6361:20042475](https://doi.org/10.1051/0004-6361:20042475)
- 605 Chandra, R. V., & Varanasi, B. S. 2015, *Python requests*  
 606 *essentials* (Packt Publishing Ltd)
- 607 Cretignier, M., Pietrow, A. G. M., & Aigrain, S. 2024,  
 608 *MNRAS*, 527, 2940, doi: [10.1093/mnras/stad3292](https://doi.org/10.1093/mnras/stad3292)
- 609 Curtis, J. L., Agüeros, M. A., Matt, S. P., et al. 2020, *ApJ*,  
 610 904, 140, doi: [10.3847/1538-4357/abbf58](https://doi.org/10.3847/1538-4357/abbf58)
- 611 Dotter, A., Chaboyer, B., Jevremović, D., et al. 2008, *The*  
 612 *Astrophysical Journal Supplement Series*, 178, 89
- 613 Dungee, R., van Saders, J., Gaidos, E., et al. 2022, *ApJ*,  
 614 938, 118, doi: [10.3847/1538-4357/ac90be](https://doi.org/10.3847/1538-4357/ac90be)
- 615 Feiden, G. A., Skidmore, K., & Jao, W.-C. 2021, *ApJ*, 907,  
 616 53, doi: [10.3847/1538-4357/abcc03](https://doi.org/10.3847/1538-4357/abcc03)
- 617 Feinstein, A., Montet, B., & Ansdell, M. 2020a, *J. Open*  
 618 *Source Softw.*, 5, 2347, doi: [10.21105/joss.02347](https://doi.org/10.21105/joss.02347)
- 619 Feinstein, A. D., Montet, B. T., Ansdell, M., et al. 2020b,  
 620 *Astron. J.*, 160, 219, doi: [10.3847/1538-3881/abac0a](https://doi.org/10.3847/1538-3881/abac0a)
- 621 Fuhrmeister, B., Czesla, S., Schmitt, J. H. M. M., et al.  
 622 2019, *A&A*, 623, A24, doi: [10.1051/0004-6361/201834483](https://doi.org/10.1051/0004-6361/201834483)
- 623 Gallet, F., Charbonnel, C., Amard, L., et al. 2017, *A&A*,  
 624 597, A14, doi: [10.1051/0004-6361/201629034](https://doi.org/10.1051/0004-6361/201629034)
- 625 García Soto, A., Newton, E. R., Douglas, S. T., Burrows,  
 626 A., & Kesseli, A. Y. 2023, *AJ*, 165, 192,  
 627 doi: [10.3847/1538-3881/acc2ba](https://doi.org/10.3847/1538-3881/acc2ba)
- 628 Grevesse, N., & Sauval, A. J. 1998, *SSRv*, 85, 161,  
 629 doi: [10.1023/A:1005161325181](https://doi.org/10.1023/A:1005161325181)
- 630 Houdebine, E. R., Mullan, D. J., Bercu, B., Paletou, F., &  
 631 Gebran, M. 2017, *ApJ*, 837, 96,  
 632 doi: [10.3847/1538-4357/aa5cad](https://doi.org/10.3847/1538-4357/aa5cad)
- 633 Irwin, A. W. 2012, *FreeEOS: Equation of State for stellar*  
 634 *interiors calculations*, *Astrophysics Source Code Library*,  
 635 record ascl:1211.002. <http://ascl.net/1211.002>
- 636 Jao, W.-C., & Feiden, G. A. 2020, *AJ*, 160, 102,  
 637 doi: [10.3847/1538-3881/aba192](https://doi.org/10.3847/1538-3881/aba192)
- 638 —. 2021, *Research Notes of the American Astronomical*  
 639 *Society*, 5, 124, doi: [10.3847/2515-5172/ac053a](https://doi.org/10.3847/2515-5172/ac053a)
- 640 Jao, W.-C., Henry, T. J., Gies, D. R., & Hambly, N. C.  
 641 2018, *ApJL*, 861, L11, doi: [10.3847/2041-8213/aacdf6](https://doi.org/10.3847/2041-8213/aacdf6)
- 642 Jao, W.-C., Henry, T. J., White, R. J., et al. 2023, *AJ*, 166,  
 643 63, doi: [10.3847/1538-3881/ace2bb](https://doi.org/10.3847/1538-3881/ace2bb)
- 644 Kislyakova, K. G., Noack, L., Johnstone, C. P., et al. 2017,  
 645 *Nature Astronomy*, 1, 878,  
 646 doi: [10.1038/s41550-017-0284-0](https://doi.org/10.1038/s41550-017-0284-0)
- 647 Kleeorin, N., Rogachevskii, I., Safiullin, N., Gershberg, R.,  
 648 & Porshnev, S. 2023, *MNRAS*, 526, 1601,  
 649 doi: [10.1093/mnras/stad2708](https://doi.org/10.1093/mnras/stad2708)
- 650 Kochukhov, O. 2021, *A&A Rv*, 29, 1,  
 651 doi: [10.1007/s00159-020-00130-3](https://doi.org/10.1007/s00159-020-00130-3)
- 652 Kumar, M., & Fares, R. 2023, *MNRAS*, 518, 3147,  
 653 doi: [10.1093/mnras/stac2766](https://doi.org/10.1093/mnras/stac2766)
- 654 Kumar, V., Rajpurohit, A. S., Srivastava, M. K.,  
 655 Fernández-Trincado, J. G., & Queiroz, A. B. A. 2023,  
 656 *MNRAS*, 524, 6085, doi: [10.1093/mnras/stad2222](https://doi.org/10.1093/mnras/stad2222)
- 657 Lammer, H., Güdel, M., Kulikov, Y., et al. 2012, *Earth*,  
 658 *Planets and Space*, 64, 179, doi: [10.5047/eps.2011.04.002](https://doi.org/10.5047/eps.2011.04.002)
- 659 Lightkurve Collaboration, Cardoso, J. V. d. M., Hedges, C.,  
 660 et al. 2018, *Astrophysics Source Code Library*,  
 661 ascl:1812.013
- 662 Mansfield, S., & Kroupa, P. 2021, *A&A*, 650, A184,  
 663 doi: [10.1051/0004-6361/202140536](https://doi.org/10.1051/0004-6361/202140536)
- 664 Middelkoop, F. 1982, *A&A*, 107, 31
- 665 Newton, E. R., Irwin, J., Charbonneau, D., et al. 2016,  
 666 *ApJ*, 821, 93, doi: [10.3847/0004-637X/821/2/93](https://doi.org/10.3847/0004-637X/821/2/93)
- 667 Nutzman, P., & Charbonneau, D. 2008, *PASP*, 120, 317,  
 668 doi: [10.1086/533420](https://doi.org/10.1086/533420)
- 669 Perdelwitz, V., Mittag, M., Tal-Or, L., et al. 2021, *VizieR*  
 670 *Online Data Catalog*, J/A+A/652/A116,  
 671 doi: [10.26093/cds/vizier.36520116](https://doi.org/10.26093/cds/vizier.36520116)
- 672 Rauscher, E., & Marcy, G. W. 2006, *PASP*, 118, 617,  
 673 doi: [10.1086/503021](https://doi.org/10.1086/503021)
- 674 Richardson, L. 2007, *April*
- 675 Robertson, P., Stefansson, G., Mahadevan, S., et al. 2020,  
 676 *ApJ*, 897, 125, doi: [10.3847/1538-4357/ab989f](https://doi.org/10.3847/1538-4357/ab989f)
- 677 Rodríguez-López, C. 2019, *Frontiers in Astronomy and*  
 678 *Space Sciences*, 6, 76, doi: [10.3389/fspas.2019.00076](https://doi.org/10.3389/fspas.2019.00076)
- 679 Rutten, R. G. M. 1984, *A&A*, 130, 353
- 680 Saar, S. H., & Linsky, J. L. 1985, *ApJL*, 299, L47,  
 681 doi: [10.1086/184578](https://doi.org/10.1086/184578)
- 682 Salvatier, J., Wiecki, T. V., & Fonnesbeck, C. 2016, *PeerJ*  
 683 *Comput. Sci.*, 2, e55, doi: [10.7717/peerj-cs.55](https://doi.org/10.7717/peerj-cs.55)
- 684 Shulyak, D., Sokoloff, D., Kitchatinov, L., & Moss, D. 2015,  
 685 *MNRAS*, 449, 3471, doi: [10.1093/mnras/stv585](https://doi.org/10.1093/mnras/stv585)
- 686 Shulyak, D., Reiners, A., Nagel, E., et al. 2019, *A&A*, 626,  
 687 A86, doi: [10.1051/0004-6361/201935315](https://doi.org/10.1051/0004-6361/201935315)
- 688 Skrutskie, M. F., Cutri, R. M., Stiening, R., et al. 2006, *AJ*,  
 689 131, 1163, doi: [10.1086/498708](https://doi.org/10.1086/498708)
- 690 Spada, F., & Lanzafame, A. C. 2020, *A&A*, 636, A76,  
 691 doi: [10.1051/0004-6361/201936384](https://doi.org/10.1051/0004-6361/201936384)
- 692 Vaughan, A. H., Baliunas, S. L., Middelkoop, F., et al.  
 693 1981, *ApJ*, 250, 276, doi: [10.1086/159372](https://doi.org/10.1086/159372)
- 694 Winters, J. G., Henry, T. J., Jao, W.-C., et al. 2019, *AJ*,  
 695 157, 216, doi: [10.3847/1538-3881/ab05dc](https://doi.org/10.3847/1538-3881/ab05dc)

<sup>696</sup> Wright, N. J., Newton, E. R., Williams, P. K. G., Drake,  
<sup>697</sup> J. J., & Yadav, R. K. 2018, MNRAS, 479, 2351,  
<sup>698</sup> doi: [10.1093/mnras/sty1670](https://doi.org/10.1093/mnras/sty1670)